ACS OMEGA

http://pubs.acs.org/journal/acsodf

Article

Efficiency of Deoxynivalenol Detoxification by Microencapsulated Sodium Metabisulfite Assessed via an *In Vitro* Bioassay Based on Intestinal Porcine Epithelial Cells

Changning Yu, Peng Lu, Shangxi Liu, Qiao Li, Erhua Xu, Joshua Gong, Song Liu,* and Chengbo Yang*

Cite This: *ACS Omega* 2021, 6, 8382−8393

Read Online

ACCESS | Metrics & More | Article Recommendations

ABSTRACT: Deoxynivalenol (DON) contamination occurs in feeds and causes a reduction in growth performance, damage to the intestinal epithelial cells, and increased susceptibility to enteric pathogen challenge. Sodium metabisulfite (SMBS) has shown promise in reducing DON; however, SMBS quickly degrades under aqueous acidic conditions such as the environment within a stomach. Thus, protection of SMBS is required for effective delivery to the small intestine to detoxify DON. This study was to encapsulate SMBS into hydrogenated palm oil-based microparticles for its delivery to the small intestine and to evaluate its efficacy on DON detoxification in simulated intestinal fluids using IPEC-J2 cells *in vitro*. The diameter of the SMBS containing microparticles was 511 ± 135 μm, and the loading capacity of SMBS in the microparticles was 45.50%; 1.41% of the encapsulated SMBS (ES) was released into the simulated gastric fluid, and 66.39% of ES was progressively released into the simulated intestinal fluid within 4 h at 37 °C. In IPEC-J2 cells, when DON was treated with the simulated gastric fluid containing 0.5% ES for 2 h, then mixed with the simulated intestinal fluid (1:1) and incubated for 2 h, cytotoxicity was not observed. DON treated with 0.5 ES decreased the gene expression of inflammatory cytokines in the cells compared with DON alone and maintained the cell integrity. To conclude, the SMBS containing microparticles were stable in the simulated gastric fluid and allowed a progressive release of SMBS in the simulated intestinal fluid. The released SMBS in the simulated intestinal fluid effectively detoxified DON.

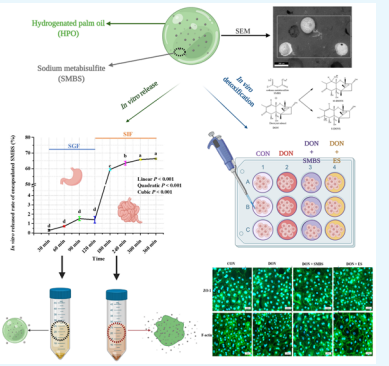

INTRODUCTION

The mycotoxin, deoxynivalenol (DON), which is produced by *Fusarium*, occurs in many commonly used cereal grains (e.g., corn, wheat, and barley). The incidence of DON contamination in grains has increased in recent years.[1] According to the latest mycotoxin report, 90% of the samples tested have shown the presence of DON.[2] The main absorption site of DON in pigs is the front part of the small intestine, and the impairments of DON consumption include digestive dysfunction (e.g., gastroenteritis, gastrointestinal tract lesions, reduced nutrient absorption), immune suppression, and reduced growth performance indices.[3−6] In addition, consuming DON-contaminated feed results in damage to the intestinal tract epithelial cells, leading to alteration of intestinal growth and barrier function as well as increased susceptibility to enteric pathogen challenge.[7,8] Therefore, different methods for effectively and economically reducing the impact of DON in food and feed ingredients have been developed, including physical, chemical, and biological approaches.[9−11] However, these different detoxification methods need to be further developed and optimized to fully realize their potential.

Sodium metabisulfite (SMBS) has been shown promising in reducing DON when added in contaminated feed.[12] It can destroy 70−100% of DON in processed grains or feeds *in vitro* with concentrations of 0.45−0.9% at pH of about 6.5.[13−16] However, SMBS is not stable and quickly degrades under aqueous acidic conditions such as in a pig stomach to form sulfur dioxide and sodium hydroxide.[17] When SMBS is mixed with diets without any protection, little SMBS can be delivered to the small intestine where an optimal pH environment exists for SMBS to detoxify DON. After reacting with SMBS at neutral pH, DON is converted to DON sulfonate (DONS), which is less toxic than DON in cell cultures.[13] Thus, there is a need to protect SMBS from degradation and deliver it to the small intestine to detoxify DON effectively.

Lipid microparticles are useful drug carriers that can be employed to deliver a variety of bioactive ingredients to the gut of animals.[18−20] Studies have shown that lipid microparticles can significantly interact with intestinal tissue and/or find utility in intestinal drug delivery.[21,22] Hydrogenated palm oil (HPO) provides a mixture of natural, even-numbered

Received: January 7, 2021
Accepted: March 10, 2021
Published: March 19, 2021

vegetable linear fatty acids, which is known for its excellent hardness at room temperature and a relatively narrow melting point.[23] The hydrogenation process reduces unsaturation, increases the melting point and solid fat content, and improves stability and oxidation resistance, thereby minimizing rancidity.[24] Meanwhile, drugs or bioactive additives encapsulated with lipids or HPO are highly tolerated (nontoxic) and can be easily produced in the industry.[25,26] Thus, the objective of this study is to develop HPO microparticles containing SMBS, which can deliver SMBS to the small intestine, and to evaluate the efficacy of DON detoxification by the microparticles in the mixture of simulated gastric fluid (SGF) and simulated intestinal fluid (SIF) using an *in vitro* intestinal epithelial cell IPEC-J2 model.

RESULTS

Size Distribution of the Lipid Microparticles. Figure 1 presents images of the lipid microparticles as well as the relative size distributions of the lipid microparticles. The microscope images showed lipid microparticles having a smooth outer shell with most appearing to have a spherical shape. The size distribution of the SMBS containing microparticles was investigated based on analyzing 220 microparticles, and the average diameter of the SMBS containing microparticles was 511 ± 135 μm.

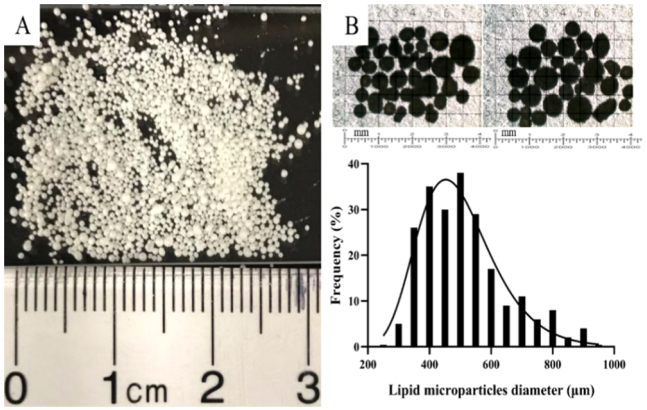

Figure 1. Microscope images of lipid microparticles (taken at 4× objective lens magnification, A) and particle size distribution (n = 220, B) of the lipid microparticles.

Characterization of the Cross Section of the Lipid Microparticles by Scanning Electron Microscope (SEM) Imaging and Energy-Dispersive X-ray Spectroscopy (EDX) Mapping. Distribution of encapsulated SMBS (ES) in lipid microparticles was evaluated to confirm that SMBS was successfully encapsulated and protected by HPO. The cross section of the lipid microparticles was observed by embedding particles within an epoxy resin and exposing the cross section by grinding and polishing so that the cross sections of some microparticles were exposed. Figure 2A shows the back-scattered electron image of ES microparticles. In the backscattering imaging, heavy elements such as sulfur and sodium appear brighter as more electrons were scattered back to the detector. Figure 2B illustrates the EDX mapping of Figure 2A. According to Figure 2B–F, the sample was characterized to have a concentrated, but uniform sulfur, sodium, and oxygen distribution within the microbead. This was represented by the bead's high density of the yellow, red, and green pigmentation, respectively. In contrast, the epoxy resin mold that embedded the sample showed no sulfur or sodium distribution, rather only carbon and oxygen. In addition, it was worth commenting that the percentages seen in Figure 2B showed the image area %, not molar %.

***In Vitro* Release of ES in SGF and SIF.** The *in vitro* release profile of SMBS from the lipid microparticles was investigated in SGF for 2 h and SIF for 4 h. The results are given in Figure 3 that 1.41% of SMBS was released in SGF for 2 h and 66.39% of loaded SMBS had progressively been released in SIF until completion, which was achieved by around 4 h.

Effects of DON on the Viability of IPEC-J2. Dose response of IPEC-J2 to DON was first studied to select an appropriate concentration of DON to further evaluate the DON detoxification efficacy by SMBS. As shown in Figure 4, cell viability decreased with the increase in the concentration of DON after incubating for 24 h ($P < 0.05$). DON at 1 μg/mL resulted in a 36.97% decrease in cell viability, and this concentration was used for the subsequent cell culture experiments.

Detoxification Efficacy of DON by SMBS in SIF. To investigate the efficacy of DON detoxification by SMBS in SIF, DON (20 μg/mL) in SGF was first incubated at 37 °C for 2 h, mixed with SIF containing SMBS at the indicated concentration, and finally incubated for an additional 2 h. Detoxification efficacy was evaluated by measuring cell viability after incubation with IPEC-J2 for 24 h. As shown in Figure 5, compared to treatments of DON with 0.125 and 0.25% SMBS, 0.5% SMBS in the mixture of SGF and SIF reduced cell cytotoxicity ($P < 0.05$). Thus, 0.5% SMBS was used for the evaluation of the efficacy of DON detoxification by ES.

Detoxification Efficacy of DON by ES. Based on the results of the *in vitro* SMBS release profile of ES microparticles, the quantity of ES in which 0.5% of SMBS released in the mixture of SGF and SIF was used to evaluate its efficacy of DON detoxification. As shown in Figure 6, the detoxification efficacy of DON by ES increased with the incubation time and 100% cell viability was achieved after incubation for 120 min in comparison to 30 min and 60 min ($P < 0.05$). Therefore, DON treated with ES for 120 min in the mixture of SGF and SIF was used in the subsequent cell culture experiment.

Effect of DON Treated with ES on the Inflammatory Response in IPEC-J2 Cells. The detoxification efficacy of ES was further evaluated through the gene expression of inflammatory cytokines. The abundances of interleukin 6 (IL-6) and interleukin 8 (IL-8) mRNAs in IPEC-J2 cells are shown in Figure 7. DON was able to induce a significant increase in gene expression of both IL-6 and IL-8 mRNA expressions in comparison to the control, SMBS, and ES treatments ($P < 0.05$). However, no significant differences were found in the relative mRNA levels of IL-6 and IL-8 among the control, SMBS, and ES treatments ($P > 0.05$).

Effect of DON Treated with ES on the Barrier Integrity in IPEC-J2 Cells. Detoxification efficacy of ES was also evaluated by measuring trans-epithelial electrical resistant (TEER). As shown in Figure 8, DON induced a significant decrease in TEER value after 24 h incubation in comparison to the control treatment ($P < 0.05$). Meanwhile, the treatments of DON and SMBS or ES showed a higher TEER than DON treatment ($P < 0.05$) and no difference was observed in TEER among the control, SMBS, and ES treatments ($P > 0.05$).

https://doi.org/10.1021/acsomega.1c00117
ACS Omega 2021, 6, 8382−8393

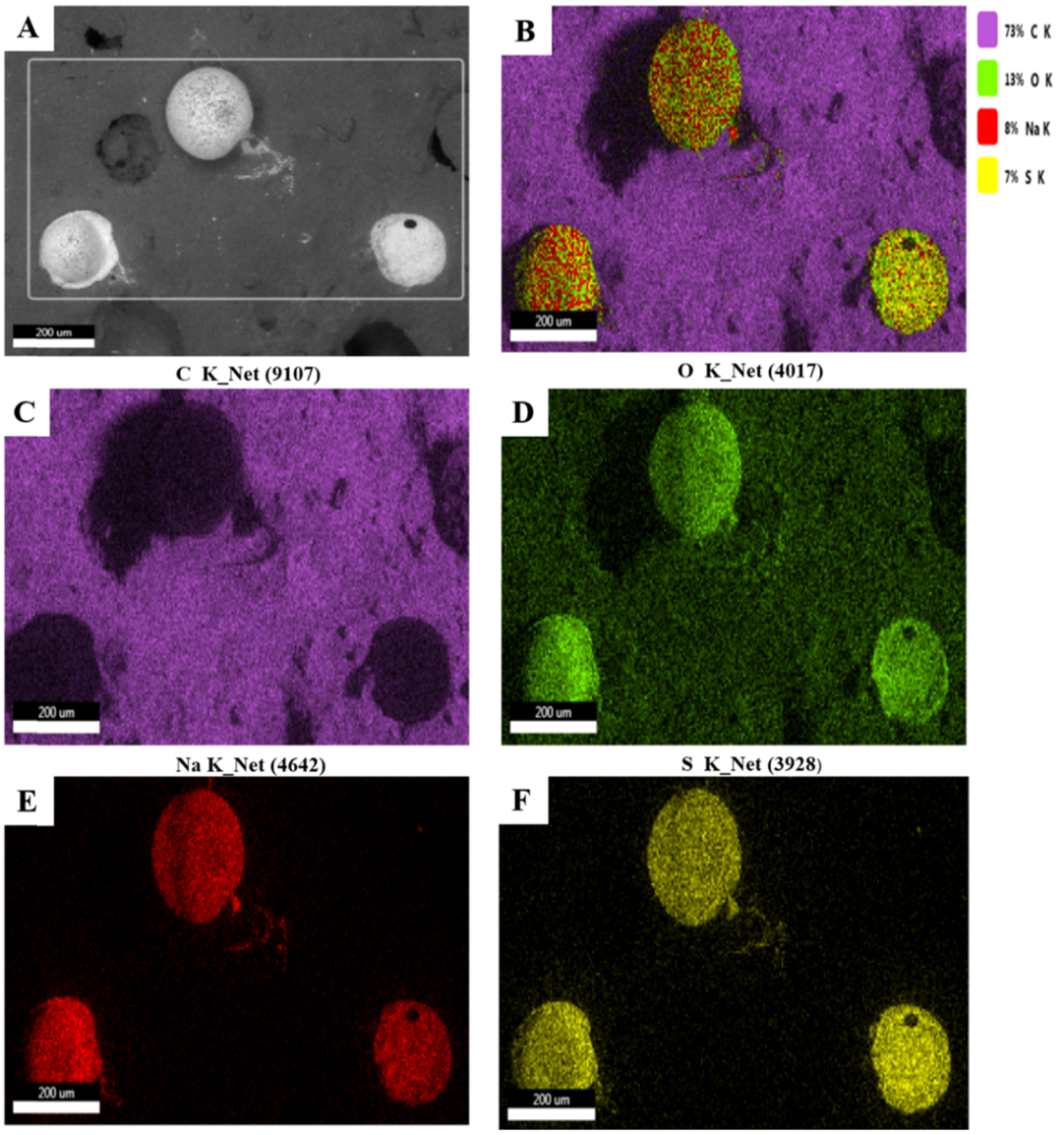

Figure 2. Scanning electron microscope (SEM) backscattered images (A) and energy-dispersive spectroscopy (EDX) mapping (B–F) of sodium metabisulfite (SMBS), carbon, oxygen, sodium, and sulfur embedded in epoxy resin.

Effect of DON Treated with ES on the Morphological Changes of Tight Junction and Cytoskeleton in IPEC-J2 Cells. As shown in Figure 9, DON treatment (1 μg/mL) resulted in zonula occludens-1 (ZO-1) proteins to curve at the cell boundaries, and these proteins were shallower in the cytoplasm. However, in the other three treatments, ZO-1 proteins were linearly distributed as z-series intercellularly or spot-like at the nuclei. Thus, in comparison, a combination of DON and SMBS or ES could protect the cells in light of the ZO-1 staining results. For filamentous actin (F-actin) staining, compared to the other three treatments, DON decreased it in the region of the cytoplasm. Simultaneously, SMBS or ES treatment with DON could preserve the regular F-actin network and resist the influence of DON under the plasma membrane and in the cytoplasm with strong green staining.

Effect of DON Treated with ES on the Gene and Protein Expression of Tight Junction Proteins in IPEC-J2 Cells. The mRNA and protein expression of ZO-1 and Occludin (OCLN) are shown in Figure 10. No significant differences were found in the relative mRNA and protein expression levels of ZO-1 among these four treatments ($P > 0.05$). However, compared to the control, DON significantly decreased the mRNA and protein expression levels of OCLN ($P < 0.05$), and SMBS and ES treatments did not affect the mRNA and protein abundance of OCLN ($P > 0.05$).

DISCUSSION

The size of the microparticles is critical in determining whether it can be used in pig feeds. Animal feed with a particle size larger than 1500 μm will rapidly settle down, resulting in a nonuniform distribution of ingredients.[27] Wen et al.[28] developed porcine epidemic diarrhea virus (PEDV)-loaded microspheres with a diameter of 700–900 μm that could effectively induce PEDV-specific mucosal immunity of pigs to PEDV. Besides, Zhang et al.[27] also tested two different sizes of capsules (250 μm and 800 μm) for intestinal delivery of carvacrol in pigs and demonstrated that increasing the size of capsules (800 μm) could deliver more carvacrol to the lower intestine of pigs. Good microparticle size ranges from 400 to 1000 μm and cannot exceed 1500 μm. Thus, ES microparticles

https://doi.org/10.1021/acsomega.1c00117
ACS Omega 2021, 6, 8382–8393

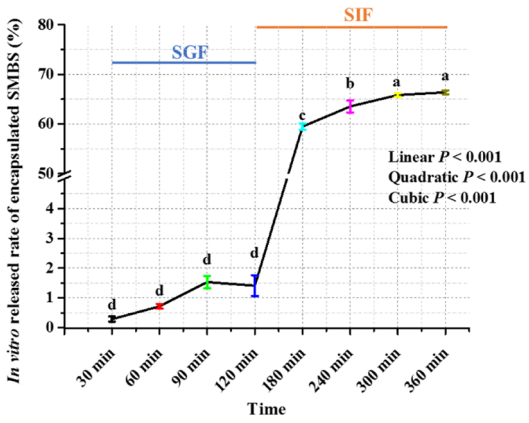

Figure 3. *In vitro* release profile of SMBS from the encapsulated SMBS (ES) microparticles in the simulated gastric fluid (SGF) and simulated intestinal fluid (SIF). Each value represents mean ± standard deviation (SD), n = 3. Note: Released rate (%) = $\frac{\text{the released SBMS}}{\text{loaded SBMS}} \times 100$; the loading capacity of ES was 45.50%; the encapsulated SMBS/SGF ratio was 0.25 g/10 mL; the encapsulated SMBS/SGF + SIF ratio was 0.25 g/20 mL.

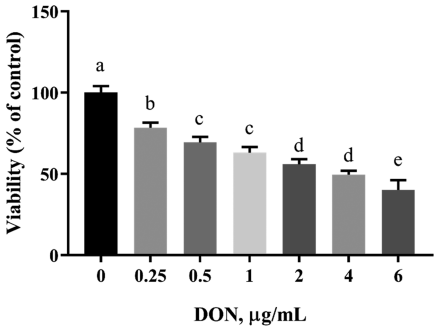

Figure 4. Effect of DON on the cell viability of IPEC-J2 cells. Note: IPEC-J2 cells were cultured in 96-well plates until 90% confluent and then treated DON at indicated concentrations for 24 h. Cell viability was measured as described in the Materials and Methods section. Data were expressed as a percentage of control (CON) and presented as mean ± SD, n = 4. Different letters indicate significant difference (P < 0.05).

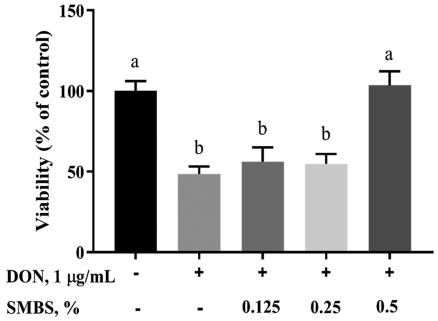

Figure 5. Effect of DON treated with SMBS on the cell viability of IPEC-J2 cells. Note: IPEC-J2 cells were cultured in 96-well plates until 90% confluent and then incubated with DON (1 μg/mL) or the same concentration of DON treated with SMBS at the indicated concentrations as described in the Materials and Methods section for 24 h. Cell viability was measured by WST-1 and expressed as a percentage of control and presented as mean ± SD, n = 4. Different letters indicate significant difference (P < 0.05).

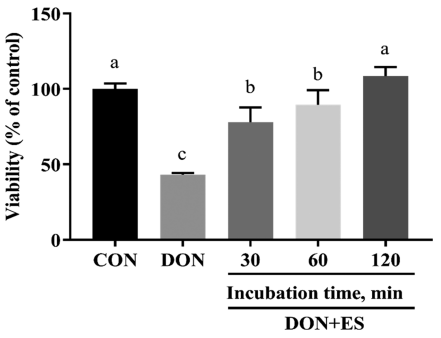

Figure 6. Effect of DON treated with encapsulated SMBS (ES) on the cell viability of IPEC-J2 cells. Note: IPEC-J2 cells were cultured in 96-well plates until 90% confluent and then incubated with DON (1 μg/mL) or the same concentration of DON treated with ES (containing 0.5% SMBS) at the indicated time as described in the Materials and Methods section for 24 h. Cell viability was measured by WST-1 and expressed as a percentage of control and presented as mean ± SD, n = 4. Different letters indicate significant difference (P < 0.05).

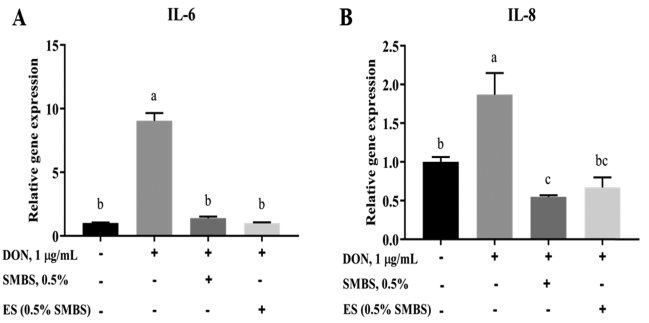

Figure 7. Effect of DON treated with SMBS or encapsulated SMBS (ES) on inflammatory response in IPEC-J2. Note: IPEC-J2 cells were cultured in 12-well plates until 90% confluent and then incubated with DON (1 μg/mL) or the same concentration of DON treated with SMBS (0.5%) or ES (containing 0.5% SMBS) (2 h) as described in the Materials and Methods section for 4 h. Total RNA was extracted, and IL-6 (A) and IL-8 (B) were measured by real-time polymerase chain reaction (RT-PCR). Data were expressed as fold change relative to control (CON) and presented as mean ± SD, n = 4. Different letters indicate significant difference (P < 0.05).

(511 ± 135 μm) in this experiment have the potential to be applied to pigs and reduce the negative effects of DON on pigs.

It has been reported that SMBS can effectively reduce the adverse impacts of DON in animal feed using either a hydrothermal treatment combined with a higher moisture content or wet preservation through the formation of the sulfonated derivative of DON, termed as DONS.[5,9,29] However, the chemical strategies of DON decontamination often require processes that may hurt the nutritional content and taste of the grain. Moreover, the SMBS remains in the feeds that may produce deleterious effects to pigs by the production of sulfur dioxide in their acidic stomach environment. Therefore, there is a need to deliver intact SMBS to the small intestine to detoxify DON effectively using innovative delivery methods. Ensuring the integrity of ES microparticles is the key to the ability to deliver SMBS to the effective site *in vivo*. HPO is a mixture of natural and even-numbered vegetable linear fatty acids, known for its excellent hardness at room temperature and a relatively narrow melting point.[23] The advantage of using hydrogenated fats to encapsulate bioactive

https://doi.org/10.1021/acsomega.1c00117
ACS Omega 2021, 6, 8382−8393

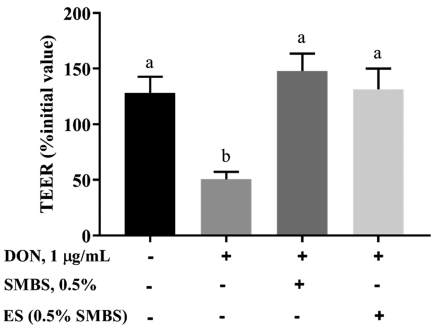

Figure 8. Effect of DON treated with SMBS or encapsulated SMBS (ES) on the trans-epithelial electrical resistance (TEER) values in IPEC-J2 cells. Note: IPEC-J2 cells were cultured in 24-well transwell inserts until reaching stable TEER and then incubated with DON (1 μg/mL) or the same concentration of DON treated with SMBS (0.5%) or ES (containing 0.5% SMBS) (2 h) as described in the Materials and Methods section for 24 h. TEER was measured before and after treatment. Data were expressed as a percentage of initial value and presented as mean ± SD, n = 3. Different letters indicate significant difference (P < 0.05).

ingredients is that it allows for a slow release of the payload while ensuring the high stability of the particles.[30,31] In this study, SMBS was encapsulated into HPO microparticles, and the protection of SMBS in SGF and release in SIF were tested by measuring the release profile in both SGF and SIF *in vitro*. The SEM and EDX results in Figure 2 indicated that SMBS was successfully encapsulated by HPO and SMBS molecules were uniformly distributed over the cross sections of the microparticles. Meanwhile, *in vitro* release experiment results suggest that SMBS could be successfully delivered to the small intestine where SMBS was released in the neutral environment by HPO encapsulation. That is because lipids are indigestible in pepsin, resulting in only 1.41% of SMBS being released within the SGF. However, lipase could readily break down the lipid matrix particles within SIF at a pH range of 6−7.[32] Bile salts in the intestinal site emulsify the broken-down lipid microparticles, thereby generating new surfaces that help facilitate the digestion of lipid matrix microparticles.[33] These findings were similar to the results of Choi et al.,[20] who reported that in the case of hydrogenated fats, 26.04% of thymol was released into the SGF, and the remaining thymol was gradually released in SIF by 24 h. Compared with this study, the SGF release in Choi's trial was slightly higher because of the solubilized thymol present on the surface of the particles. However, through SEM/EDX analysis and *in vitro* release test, we found that the SMBS was well encapsulated into HPO in this study and only 1.41% of SMBS was released in the SGF. Therefore, the results of the present study demonstrated that ES microparticles by HPO could potentially and efficiently deliver SMBS to the small intestine *in vivo*.

DON has been reported to be toxic to intestinal epithelial cells, and the reaction products of DON and SMBS (DON sulfonates, DONS) were less toxic compared with DON.[17] *In vitro* viability assay has been used to evaluate the cytotoxicity of DON using intestinal porcine epithelial cell line IPEC-1 and IPEC-J2.[13,34] These two cell lines are derived from the small intestines of pigs. The nontransformed jejunum intestinal cell line IPEC-J2 is the best reasonable porcine epithelial cell culture model in comparison to IPEC-1 since it maintains most of its epithelial nature.[35] Dänicke et al.[13] indicated that the IC_{50} of DONS was 17 μM, which was lower than that of DON estimated at 2.97 μM under the same conditions. In this study, we used the IPEC-J2 cells to test the detoxification efficiency of ES in the mixture of SGF and SIF on DON and applied the IPEC-J2 cells to investigate the cytotoxicity and detoxification efficacy of DON induced by SMBS. A dose-dependent cytotoxicity of DON was first tested by measuring its viability using WST-1 assay. Compared to other cell viability assays, WST-1 is a tetrazolium salt that produces a highly water-soluble formazan by mitochondrial dehydrogenase enzymes and no additional dissolution step is required to dissolve the formazan.[36] Furthermore, WST-1 also do not interfere with phenol red or other culture mediums.[37] We found that 1 μg/mL of DON (3.3 μM) could cause a 36.97% viability decrease after incubating for 24 h, which was consistent with the previous study.[13] Therefore, 1 μg/mL of DON was used to

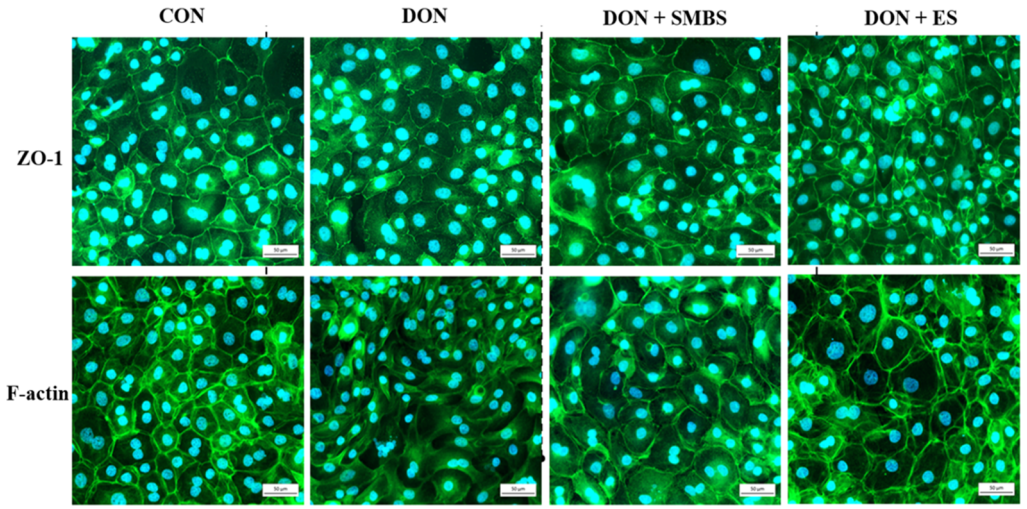

Figure 9. Effect of DON treated with SMBS or encapsulated SMBS (ES) on the morphological changes of tight junction and cytoskeleton in IPEC-J2 cells. Note: IPEC-J2 cells were cultured on coverslips in 24-well plates for 1 week until tight junction was formed and then incubated with DON (1 μg/mL) or the same concentration of DON treated with SMBS (0.5%) or ES (containing 0.5% SMBS) (2 h) as described in the Materials and Methods section for 24 h. Cells were fixed and stained with tight junction protein zonula occludens-1 (ZO-1) and filamentous actin (F-actin) as described in the Materials and Methods section, and representative images were presented. Scale bar represents 50 μm.

https://doi.org/10.1021/acsomega.1c00117
ACS Omega 2021, 6, 8382−8393

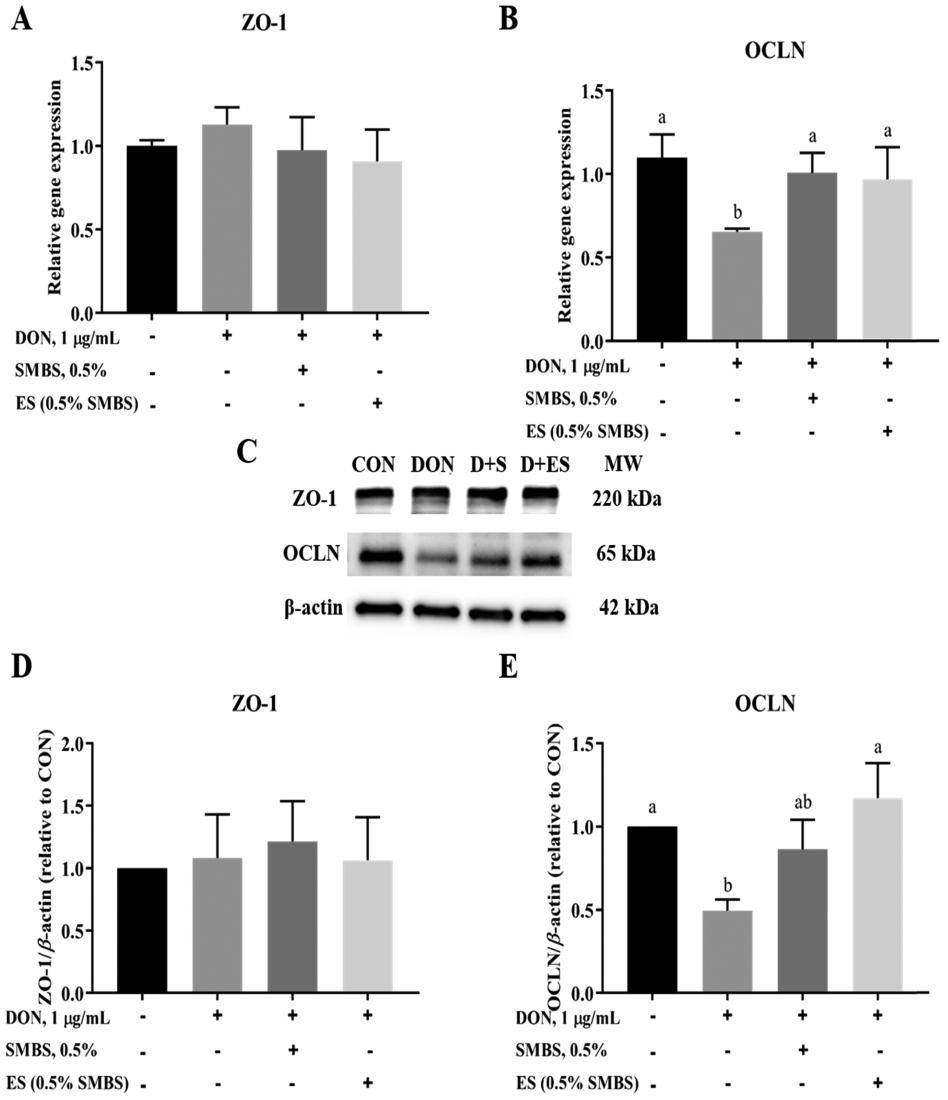

Figure 10. Effect of DON treated with SMBS or encapsulated SMBS (ES) on the gene and protein expression of tight junctions in IPEC-J2 cells. Note: IPEC-J2 cells were cultured in 12-well plates (for gene expression) or 6-well plates (for protein expression) until 90% confluent and then incubated with DON (1 μg/mL) or the same concentration of DON treated with SMBS (0.5%) or ES (containing 0.5% SMBS) (2 h) as described in the Materials and Methods section for 4 h (for gene expression) or 24 h (for protein expression). Total RNA and protein were extracted. Gene expression of zonula occludens-1 (ZO-1) (A) and occludin (OCLN) (B) was measured by RT-PCR, and data were expressed as fold change relative to control (CON) and presented as mean ± SD, $n = 4$. Different letters indicate significant difference ($P < 0.05$). Protein expression of ZO-1 (D) and OCLN (E) was detected by Western blot analysis, and representative images (C) were presented. CON: control; D + S: DON treated with SMBS; D + ES: DON treated with encapsulated SMBS.

evaluate detoxification efficacy by SMBS in this study. Then, we found that the cytotoxicity of DON did not significantly change after incubating for 2 h in SGF and another 2 h incubation in the mixture of SGF and SIF, which suggested that DON-contaminated feed could tolerate the acidic condition in the stomach and exert cytotoxicity to the epithelial cells in the small intestine. Similar results were obtained by Lauren et al. and Wolf et al.,[38,39] who reported that DON was relatively stable in buffer solutions with a pH range of 1−7. However, Mishra et. al.[40] investigated that DON was unstable in acidic condition and determined that around 30% of DON decreased after incubating for 1 h at pH 3 using high-performance liquid chromatography (HPLC) assay. The difference in results may be due to different processing conditions, or perhaps the difference may be due to different measurement techniques. Meanwhile, the efficiency of SMBS to detoxify DON in the mixture of SGF and SIF solution was examined. The amounts of SMBS (0.5−1%) added in the feeds has been reported to efficiently detoxify DON in the feed.[16,17] The ratio of SMBS to DON was approximately 900 mg SMBS/mg DON that has been suggested to reduce more than 95% of DON contaminated in the feed.[17] In this study, 0.5% of SMBS in the mixture of SGF and SIF could efficiently detoxify DON at a concentration of 20 mg/L. Interestingly, the ratio of SMBS to DON is 500 mg SMBS/mg DON in this study, which is almost 2 times lower than the previous *in vitro* detoxification for the contaminated feed.[17] The possible reason is that the cell culture trial is only for a single DON, and *in vivo* contaminated feed detoxification will consume SMBS by other mycotoxins. Therefore, ES containing equivalent SMBS was incubated with the same concentration of DON first in the SGF for 2 h and then mixed with SIF at a ratio of 1:1 and

https://doi.org/10.1021/acsomega.1c00117
ACS Omega 2021, 6, 8382−8393

incubated for up to 2 h. In addition, ES could efficiently detoxify DON in the mixture of SGF and SIF, suggesting that encapsulation could protect SMBS from the acidic stomach condition and deliver SMBS to the small intestine. Meanwhile, according to the results of 4 h incubation in SIF in Figure 3, the complete release of all SMBS from ES microparticles was not observed, and only 64.98% of SMBS was released from ES microparticles. However, *in vitro* DON detoxification performance by DON+SMBS and DON+ES treatments, as shown in Figures 7−10, resulted in no significant difference. The reason is that the pure SMBS (0.5%) could be partially degraded due to dissolution in the SGF and SIF, but the ES microparticles (0.32%) could achieve the same effect as pure SMBS due to the protective effect of HPO in 2 h incubation. Thus, if one simply adds pure SMBS into animal feeds, only a small quantity of SMBS could be delivered to the DON digestion and absorption site in pigs. In the present study, SMBS was encapsulated into HPO to protect SMBS from the acidic gastric fluid and delivered to the intestinal site where SMBS can fully function.

DON affects the integrity of the intestinal barrier and induces the abnormal expression of proinflammatory cytokines in IPEC-J2 cells.[41−43] In this study, the inflammation induced by DON was evaluated by measuring the gene expression of the proinflammatory cytokine IL-6 and IL-8, which were similar to the results of Wang et al.[42] Meanwhile, we found that DON treated with either SMBS or ES in the incubations with SGF and SIF did not increase the expression of both IL-8 and IL-6, which is another evidence supporting that the released SMBS in the SIF effectively detoxified DON.

TEER is a well-established and widely accepted quantitative technique for measuring the integrity of tight junction dynamics in endothelial and epithelial monolayer cell culture models.[44] Before evaluating the transport of drugs or chemicals, the TEER value is a powerful indicator of cell barrier integrity. In the present study, DON detoxification efficacy by SMBS and ES was also tested by measuring TEER. The results illustrated that the effect of SMBS and ES showed a higher TEER than DON treatment and no difference was observed in TEER between control, SMBS, and ES treatments, suggesting that DON treated with ES could maintain its barrier integrity.

Tight junction proteins play a crucial role in sealing the intercellular space between epithelial cells, thus the epithelial barrier.[45] Paracellular transport of luminal antigens was prevented as a result of a meshlike network of tight junction proteins that form on the surface of the lumen. The tight junction protein network is composed of transmembrane proteins with extracellular domains that cross plasma membranes, thus interacting with adjacent cells and cytoplasmic scaffolding within the cells. The transmembrane portion of tight junction proteins contains OCLN, claudins (CLDNs), junctional adhesion molecules, and tricellulin, which combine to form a barrier at the apical−lateral membrane within the epithelial cells. On the other hand, cytoplasmic scaffolding of tight junction proteins such as ZOs allows a linkage between transmembrane tight junction proteins and the actin cytoskeleton.[46,47] Tight junction protein mRNA expression correlates with ongoing repair mechanisms within established epithelial cell monolayers; however, assessment of tight junction proteins should not be limited to the gene level, as mRNA concentration does not necessarily correlate with the protein level.[48,49] To further validate the efficacy of ES, we demonstrated that DON treated with ES could maintain the morphological integrity of tight junction proteins and its cytoskeleton and the gene and protein expressions of OCLN.

CONCLUSIONS

The lipid microparticles containing SMBS were both smooth and spherical, and the SMBS was clearly shown in the center of microparticles, covered by HPO in the EDX mapping. The ES microparticles were stable in the SGF and allowed a progressive release of SMBS in the SIF. Moreover, the released SMBS in the SIF effectively detoxified DON, which was evidenced by fewer adverse effects to the intestinal epithelial cells. Therefore, these microparticles could be used in pig feeds to detoxify DON. However, the efficacy of DON detoxification by microparticles needs to be further investigated with pig experiments.

MATERIALS AND METHODS

Materials. DON (D0156), pepsin-derived from porcine gastric mucosa (≥250 units/mg), pancreatin originated from porcine pancreas (≥3 USP), sodium hydroxide (ACS reagent, ≥97%), ammonium carbonate (ACS reagent, ≥30%), and calcium chloride dehydrate (BioXtra, ≥99.0%) were purchased from the Sigma-Aldrich (Oakville, ON, Canada). SMBS was provided by the company (Yueyang Sanxiang Chemical Co., Ltd, Hunan, China). Hydrogenated palm oil was purchased from Hangzhou Kangdequan Feed Co., Ltd., Zhejiang, China. Potassium phosphate monobasic (ACS reagent, 99.0%), sodium chloride (99.0%), potassium chloride (99.0%), sodium bicarbonate (99.5%), and hydrochloric acid (ACS reagent, 35−38%) were purchased from Fisher Scientific (Oakville, ON, Canada). Epoxy resin (Cat. No. EP-3000-128), epoxy hardener (Cat. No. EH-3000-32), silicon carbide waterproof paper (Grit size: 600 and 240), 6 μm DIAMAT (250 mL) polycrystalline diamond high viscosity (Cat. No. PC-1006-250), 3 μm DIAMAT (250 mL) polycrystalline diamond high viscosity (Cat. No. PC-1003-250), 1 μm DIAMAT (250 mL) polycrystalline diamond high viscosity (Cat. No. PC-1001-250), and diamond grinding particles (6, 3, and 1 μm) were purchased from PACE Technologies (Tucson, AZ, America). Nova NanoSEM 450 was purchased from AMETEK EDAX (New Jersey, NJ), and an optical microscope (EVOS XL Core) was provided from Thermo Fisher Scientific (Mississauga, ON, Canada). A microscale was provided by I-SEEINGTM, Shanghai QingYing E&T LLC (Pudong, Shanghai, China).

Microparticles Preparation. A balance scale was used to weight 65% (w/w) of SMBS, 35% (w/w) of corn starch, and 10% (w/w) of distilled water; they were mixed at room temperature in a feed mixing machine (Lanxi Huafeng Engineering Machinery Manufacturing Co., Ltd, Zhejiang, China) for 10 min, followed by extrusion with a 60-mesh sieve and granulation with a 30-mesh sieve. Afterward, 30% (w/w) of HPO was weighed and dissolved in 18 L of ethanol to yield an encapsulated solution. Placed 70% (w/w) of the granules obtained in the above step in a BLF-500 fluidized bed (Hangzhou Kangdequan Feed Co., Ltd., Zhejiang, China) with a flow rate of 0.1 L/min, an inlet air temperature of 80°C, and an outlet air temperature at room temperature. The coating process was carried out for 3 h, and the product particle size was above 85% through a 20-mesh sieve. Finally, dried lipid microparticles were stored in airtight plastic bags.

https://doi.org/10.1021/acsomega.1c00117
ACS Omega 2021, 6, 8382−8393

SMBS Quantification. SMBS was quantified using Ellman's reagent as described by Sadegh et al.[50] Briefly, the samples were diluted to appropriate concentrations and 250 μL of diluted sample was mixed with 50 μL of Ellman's reagent and 2.5 mL of reaction buffer (0.1 M sodium phosphate, pH 8.0, containing 1 mM EDTA) and incubated at room temperature for 15 min. The absorbance at 412 nm was measured using a Synergy H4 Hybrid Multi-Mode Microplate Reader (BioTek, Winooski, VT). The concentrations of SMBS were calculated based on the standard curve of SMBS prepared. The final microparticles contained 45.5% of SMBS, 24.5% of corn starch, and 30% of HPO.

Diameter and Size Distribution of Lipid Microparticles. Images of the particle size distribution for the lipid microparticles were taken by an EVOS XL core optical microscope. The diameter of the lipid microparticles was manually determined using ImageJ software, from the photo images using a ruler and a microscale (I-SEEINGTM, Shanghai QingYing E&T LLC, Pudong, Shanghai, China) according to ref 51. The length of each grid (Figure 1B) in the microscale was 500 μm.

Preparation of Lipid Microparticles Embedded in Epoxy Resin. The lipid microparticles were embedded in commercially available epoxy resin to expose the cross section to observe the encapsulated bioactive ingredients. The embedded lipid microparticle samples were prepared using a mold (diameter: 2.0 cm, height: 3.0 cm). The epoxy resin (Cat. No. EP-3000-128) and epoxy hardener (Cat. No. EH-3000-32) were mixed using a 5:1 ratio by weight. Then, the resin mixture was poured into the mold and the lipid microparticles were dispersed in the resin mixture by slowly stirring without any bubbles. The lipid microparticle samples in the resin mixture were kept at room temperature for 24 h to allow hardening. The embedded samples were polished by a grinding/polishing machine (Ecomet 3, Buehler) using a silicon carbide waterproof paper (Grit size 240) first and then using a silicon carbide waterproof paper (Grit size 600) to expose the cross section of the lipid microparticles. Water was sprayed on the surface sample (up to 100 mL) during the grinding/polishing process to prevent excessive temperatures on the surface of the samples. Between each grinding/polishing process, the samples were washed with distilled water and sonicated for 5 min. Diamond grinding particles with micron sizes of 6, 3, and 1 μm were then used to polish the surface of the cross-sectioned microparticles with 3−5 mL of 6 μm DIAMAT (250 mL) polycrystalline diamond high viscosity, 3 μm DIAMAT (250 mL) polycrystalline diamond high viscosity (Cat. No. PC-1003-250), and 1 μm DIAMAT (250 mL) polycrystalline diamond high viscosity (Cat. No. PC-1001-250). After these processes, the samples' surfaces were rewashed by sonication with distilled water for 5 min.

Characterization of the Cross Section of Lipid Microparticles by SEM Imaging and EDX Mapping. The distributions of bioactive ingredients in the lipid microparticles were tested using an SEM imagery and EDX mapping. The SEM instrument was equipped with a concentric (insertable) higher-energy electron detector, circular backscattering (CBS), and an octane super silicon drift detector (SDD) and was operated at 100 Pa and an accelerating voltage of 10 kV. The EDX mapping was processed at a resolution of 256 × 200 for 30 min.

***In Vitro* Release of Encapsulated SMBS in SGF and SIF.** The *in vitro* release profile of SMBS in the lipid microparticles was determined using SGF for 2 h and SIF for 4 h. Both SGF and SIF were prepared according to the methods described by Minekus et al.[52] with some modifications. The SGF contained 47.2 mmol/L NaCl, 25 mmol/L $NaHCO_3$, 6.9 mmol/L KCl, 0.9 mmol/L KH_2PO4, 0.5 mmol/L $(NH_4)_2CO_3$, 0.1 mmol/L $MgCl_2(H_2O)_6$, 0.15 mmol/L $CaCl_2$ $(H_2O)_2$, and 2000 U/mL pepsin originated from porcine gastric mucosa. The SIF contained 85 mmol/L $NaHCO_3$, 38.4 mmol/L NaCl, 6.8 mmol/L KCl, 0.8 mmol/L KH_2PO_4, 0.33 mmol/L $MgCl_2(H_2O)_6$, 0.6 mmol/L $CaCl_2(H_2O)_2$, 10 mM bile salts, and 1% (by volume) pancreatin originated from porcine pancreas.[53] The pH of SGF and SIF was adjusted to 3.0 and 7.0, respectively, using 1 M HCl or NaOH.

For the detection of the SMBS release profile in SGF, 10 mL of 2.5% pure ES in prewarmed SGF (37 °C) was incubated at 37 °C with shaking for up to 120 min. Samples were taken at 30 min, 60 min, 90 min, and 120 min, and the SMBS concentrations were measured immediately.

For the detection of SMBS release profile in SIF, 10 mL of 2.5% pure ES in prewarmed SGF (37 °C) was first incubated at 37 °C with shaking for 120 min and then mixed with an equal volume of prewarmed SIF (37 °C) and pH was adjusted to 7.0 by either 1 M HCl or NaOH. The mixtures were then incubated at 37 °C with shaking for up to 240 min. The samples were taken at 60 min (SGF 120 min + SIF 60 min), 120 min (SGF 120 min + SIF 120 min), 180 min (SGF 120 min + SIF 180 min), and 240 min (SGF 120 min + SIF 240 min). SMBS concentrations were measured immediately as described in the following section. The *in vitro* release profile experiment was conducted in triplicate.

***In Vitro* Detoxification of DON by SMBS and ES Microparticles in SGF and SIF.** SGF (pH 3) containing 1% pepsin (≥250 units/mg, Sigma-Millipore) and SIF (pH 7) containing 1% pancreatin (≥3 USP, Sigma-Millipore) and 10 mM bile salt (Sigma-Millipore) were prepared following the formulation described by Minekus et. al.[52] For *in vitro* detoxification of DON by SMBS, DON (20 μg/mL) in SGF was incubated at 37 °C with shaking for 2 h and then mixed with SIF containing 0.25, 0.5, and 1% SMBS at the ratio of 1:1 to achieve a final concentration of SMBS at 0.125, 0.25, and 0.5% in the mixture with pH adjusted to 7. The mixture was then incubated at 37 °C with shaking for another 2 h and sterilized by passing through a syringe filter (0.22 μM). The mixture was diluted 10 times with medium (1 μg/mL of DON) and was used for cell treatment. Cell viability was assessed by the water-soluble tetrazolium salts (WST-1) (Sigma-Millipore) after a 24 h treatment. For *in vitro* detoxification of DON by ES microparticles in SGF and SIF, the process was the same as the detoxification of DON by SMBS *in vitro*.

Cell Culture. The nontransformed neonatal jejunal epithelial cell line IPEC-J2 was grown in DMEM-Ham's F-12 (1:1) (Fisher Scientific, Ottawa, ON, Canada) supplemented with 5% fetal bovine serum (FBS) (Hyclone, Canadian Origin; Fisher Scientific, Ottawa, ON, Canada), 3 ng/mL recombinant human epithelial growth factor (EGF) (Fisher Scientific, Ottawa, ON, Canada), penicillin (100 IU/mL), streptomycin (100 μg/mL), and 0.25 μg/mL of amphotericin B (Fisher Scientific, Ottawa, ON, Canada), and maintained in an atmosphere of 5% carbon dioxide (CO_2) at 37 °C for cultures and assays. The culture medium was replaced every 2 days.

https://doi.org/10.1021/acsomega.1c00117
ACS Omega 2021, 6, 8382−8393

Table 1. Primers for Real-Time PCR Analysis

genes	GenBank ID	primer sequence (5′−3′)	product size (bp)	references
IL-6	NM_214399.1	AAGGTGATGCCACCTCAGAC	151	56
		TCTGCCAGTACCTCCTTGCT		
IL-8	NM_213867.1	CACCTGTCTGTCCACGTTGT	126	56
		AGAGGTCTGCCTGGACCCCA		
ZO-1	NM_001355013.1	GATCCTGACCCGGTGTCTGA	200	56
		TTGGTGGGTTTGGTGGGTT		
OCLN	XM_017008914.2	GACTATGTGGAAAGAGTTGAC	174	57
		ACCGCTGCTGTAACGAG		
CycA	NM_214353.1	GCGTCTCCTTCGAGCTGTT	160	
		CCATTATGGCGTGTGAAGTC		

[a]Note: IL-8, interleukin 8; IL-6, interleukin 6; ZO-1, zonula occluden-1; OCLN, occluding; CycA, cyclophilin-A.

Viability Assay. Cell viability was measured using the WST-1 Cell Proliferation Reagent (Sigma-Aldrich, Roche, Indianapolis, IN) according to the manufacturer's instructions. Briefly, IPEC-J2 cells were seeded into 96-well plates (Corning Costar, New York City, NY) at a density of 1×10^4 cells/mL and cultured until 90% confluent. The cells were then incubated with DON (1 μg/mL) or the same concentration of DON detoxified by SMBS for 24 h. After incubation, the cells were washed twice with PBS and 100 μL fresh culture medium containing 10% WTS-1 was added and incubated for 1 h. Untreated cells with 0 μg/mL of DON and 0% of SMBS were used as the control group. The absorbance at 450 nm was measured using a Synergy H4 Hybrid Multi-Mode Microplate Reader (BioTek, Winooski, VT). Cell viability was presented as a percentage of untreated control cells. All of the treatment groups were under the same condition, and the sample wells were randomly assigned into each treatment group.

Inflammation Induction. To study DON-induced inflammation, IPEC-J2 cells were cultured in 12-well plates until 90% confluent. The cells were then stimulated with DON (1 μg/mL) or DON detoxified by SMBS or ES as described above for 3 h. Untreated cells (with 0 μg/mL of DON and 0% of SMBS) were used as the control group. After treatments, RNA was extracted and proinflammatory gene expression assays were analyzed by real-time PCR (RT-PCR).

Total RNA was extracted from IPEC-J2 cells using Trizol reagents (Invitrogen) following the manufacturer's protocol. RNA concentration, OD260/OD280, and OD260/OD230 were analyzed by a Nanodrop-2000 spectrophotometer (Thermo Scientific, Ottawa, ON, Canada). The integrity of RNA was verified by agarose gel electrophoresis. Total RNA (1 μg) was reverse-transcribed into cDNA using an iscriptTM cDNA Synthesis kit (Bio-Rad, Mississauga, ON, Canada) following the manufacturer's instruction. Quantitative RT-PCR was performed using SYBR Green Supermix (Bio-Rad, Mississauga, ON, Canada) on a CFX Connect RT PCR Detection System (Bio-Rad, Mississauga, ON, Canada). The primers for RT-PCR analysis were designed with Primer-Blast based on the published mRNA sequence in the GenBank. All of the primers spanned at least two exons. The sequences of primers are listed in Table 1. The thermal profile for all of the reactions was 3 min at 95 °C, 40 cycles of 20 s at 95 °C, 30 s at 60 °C, and 30 s at 72 °C. At the end of each cycle, the fluorescence monitoring was for 10 s. Each reaction was completed with a melting curve analysis to ensure the specificity of the reaction. RT-PCR data were analyzed using the $2^{-\Delta\Delta CT}$ method to calculate the relative fold change of target genes using cyclophilin-A (CycA) as the reference gene.[54,55]

TEER Measurement. The TEER measurements on cell monolayers were made using a Millicell Electrical resistance system (ESR-2) (Millipore-Sigma) as described before.[56] Briefly, IPEC-J2 cells were seeded into Millicell membrane cell inserts (24 wells, Corning Costar, New York City, NY) at a density of 1×10^5 cells/cm^2 and TEER was monitored every other day. When the monolayer was completely differentiated, the cells were treated with control, DON (1 μg/mL), or DON detoxified by SMBS (0.5%) or ES (containing 0.5% SMBS) for 24 h. TEER was measured before and after treatments, respectively. The data were presented as a percentage of initial values before treatments.

Immunofluorescence Staining. Cells were cultured on coverslips (Fisher Scientific, Ottawa, ON, Canada) for 1 week and then treated with control, DON (1 μg/mL) or DON detoxified by SMBS (0.5%) or ES (containing 0.5% of SMBS) for 24 h. After treatments, the cells were fixed with 4% paraformaldehyde (PFA) (Sigma, Oakville, ON, Canada). The cells were first blocked with 5% goat serum (Jackson ImmunoResearch Laboratories, West Grove, PA) for 1 h at room temperature and then incubated with rabbit anti-ZO-1 polyclonal antibody (1:100 dilution, Thermo Scientific) at 4 °C overnight. The cells were washed three times with PBS and incubated with Alexa fluor 488 goat anti-rabbit (Thermo Scientific, Cat. No. A-11034) for 1 h at room temperature. After three washes with PBS, the cells were mounted with Vectashield Mounting Medium with DAPI (Vector Laboratories, Burlingame, CA) and images were taken on a Zeiss fluorescence microscope (Carl Zeiss Canada Ltd, Toronto, ON, Canada).

Western Blot Analysis. The specific primary antibodies against ZO-1 (from rabbit, Thermo Scientific, Cat. No. 61-7300) and OCLN (from rabbit, Thermo Scientific, Cat. No. 71-1500) were purchased from Thermo Scientific (Ottawa, ON, Canada). β-Actin (from mouse, Thermo Scientific, Cat. No. AM4302) was used as the internal reference. Cells were cultured in a six-well plate at a seeding density of 4×10^5 cells/well. According to the instructions of protein extraction kit (Thermo Scientific, Ottawa, ON, Canada), total protein was extracted as described before.[57] The bicinchoninic acid (BCA) protein detection kit (Thermo Scientific, Ottawa, Ontario, Canada) was utilized for quantifying a portion of the protein. The protein was then heat-denatured in an SDS-PAGE loading buffer. Subsequently, proteins were electrophoresed on polyacrylamide gels and electro-transferred to micro nitrocellulose membranes (Bio-Rad, Laboratories Ltd., Montreal,

https://doi.org/10.1021/acsomega.1c00117
ACS Omega 2021, 6, 8382−8393

QC, Canada). The immune response was carried out by the following steps: first, incubate the membrane, then block with 5% nonfat dry milk in Tris-buffered saline including 0.1% Tween 20 (TBST), then combine with rabbit anti-ZO-1 (Thermal Scientific, Cat. No. 61-7300) and rabbit anti-OCLN (Thermal Scientific, Cat. No. 71-1500), and left to dilute the protein overnight at 4 °C (1:1000, Abcam, Inc., Toronto, Canada). After that, the membrane was washed with TBST every 10 min five times. The horseradish peroxidase-conjugated secondary antibody (1:5000, goat anti-rabbit, Jackson ImmunoResearch Laboratories) was used for the detection of the immune complexes, and then the membrane was washed five times with TBST for 5 min each. The Clarity TM Western ECL Substrate was applied to the blot following the manufacturer's recommendations (Bio-Rad, Laboratories Ltd., Montreal, QC, Canada). The chemiluminescent signals were captured using a ChemiDoc MP imaging system (Bio-Rad, Laboratories Ltd., Montreal, QC, Canada), and the band intensities were qualified by ImageLab 6.0 (Bio-Rad, Laboratories Ltd., Montreal, QC, Canada). All protein measurements were normalized to β-actin protein, and all of the data were expressed as relative to those values from the treatment and control.[58]

Statistical Analysis. The diameter of lipid microparticles was analyzed by ImageJ software. The representative data from one of the three independent experiments were used for statistical analysis. Each well from a multiwell plate was used as the experimental unit for all analyses. For the cell viability, gene expression, and tight junction protein expression, each treatment had four replicates. For the TEER values, each treatment had three replicates. All of the treatment groups were under the same condition, and the sample wells were randomly assigned to each treatment group. Data were presented as mean ± standard deviation (SD). Data were analyzed using GraphPad Prism 8.0, and the difference between groups was compared with one-way analysis of variance (ANOVA) followed by Tukey's multiple comparisons. $P < 0.05$ was considered a significant difference.

AUTHOR INFORMATION

Corresponding Authors

Song Liu − *Department of Biosystems Engineering, University of Manitoba, Winnipeg, Manitoba R3T 2N2, Canada;* orcid.org/0000-0003-0301-9535; Email: Song.liu@umanitoba.ca

Chengbo Yang − *Department of Animal Science, University of Manitoba, Winnipeg, Manitoba R3T 2N2, Canada;* orcid.org/0000-0003-4449-5132; Email: chengbo.yang@umanitoba.ca

Authors

Changning Yu − *Department of Biosystems Engineering, University of Manitoba, Winnipeg, Manitoba R3T 2N2, Canada*

Peng Lu − *Department of Animal Science, University of Manitoba, Winnipeg, Manitoba R3T 2N2, Canada*

Shangxi Liu − *Department of Animal Science, University of Manitoba, Winnipeg, Manitoba R3T 2N2, Canada*

Qiao Li − *Department of Animal Science, University of Manitoba, Winnipeg, Manitoba R3T 2N2, Canada*

Erhua Xu − *King Techina Group, Hangzhou 311107, China*

Joshua Gong − *Guelph Research and Development Centre, Agriculture Agri-Food Canada, Guelph, Ontario N1G 5C9, Canada*

Complete contact information is available at: https://pubs.acs.org/10.1021/acsomega.1c00117

Notes

The authors declare no competing financial interest.

ACKNOWLEDGMENTS

The present study was supported by the Canadian Swine Research and Development Cluster III (Agriculture and Agri-Food Canada, #1794), Manitoba Pork Council (C. Yang, 50832), the Natural Sciences and Engineering Research Council of Canada (NSERC) Discovery Grant (RGPIN-2019-06094), and Canada Foundation for Innovation. The authors thank Fernando Esposito and Dr. Paula Azevedo for their help in preparing the manuscript.

ABBREVIATIONS USED

DON, deoxynivalenol; DONS, deoxynivalenol sulfonate; SMBS, sodium metabisulfite; HPO, hydrogenated palm oil; SEM, scanning electron microscope; EDX, energy-dispersive spectroscopy; CBS, circular backscattering; SDD, silicon drift detector; ES, encapsulated SMBS; SGF, simulated gastric fluid; SIF, simulated intestinal fluid; IPEC-J2, intestinal epithelial cell; WST-1, water-soluble tetrazolium salts; CO2, carbon dioxide; TEER, trans-epithelial electrical resistance; CycA, cyclophilin-A; ESR-2, electrical resistance system; IL-8, interleukin 8; IL-6, interleukin 6; ZO-1, zonula occluden-1; F-actin, filamentous actin; OCLN, occludin; CLDNS, claudins; EGF, epithelial growth factor; FBS, fetal bovine serum; PFA, paraformaldehyde; SD, standard deviation; PEDV, porcine epidemic diarrhea virus; HPLC, high-performance liquid chromatography

REFERENCES

(1) Smith, M. C.; Madec, S.; Coton, E.; Hymery, N. Natural co-occurrence of mycotoxins in foods and feeds and their in vitro combined toxicological effects. *Toxins* **2016**, *8*, No. 94.

(2) Foroud, N. A.; Baines, D.; Gagkaeva, T. Y.; Thakor, N.; Badea, A.; Steiner, B.; Bürstmayr, M.; Bürstmayr, H. Trichothecenes in cereal grains-an update. *Toxins* **2019**, *11*, No. 634.

(3) Grenier, B.; Applegate, T. J. Modulation of intestinal functions following mycotoxin ingestion: Meta-analysis of published experiments in animals. *Toxins* **2013**, *5*, 396−430.

(4) Pinton, P.; Oswald, I. P. Effect of deoxynivalenol and other Type B trichothecenes on the intestine: a review. *Toxins* **2014**, *6*, 1615−1643.

(5) Young, J. C.; Subryan, L. M.; Potts, D.; McLaren, M. E.; Gobran, F. H. Reduction in levels of deoxynivalenol in contaminated wheat by chemical and physical treatment. *J. Agric. Food Chem.* **1986**, *34*, 461−465.

(6) Döll, S.; Dänicke, S. The Fusarium toxins deoxynivalenol (DON) and zearalenone (ZON) in animal feeding. *Prev. Vet. Med.* **2011**, *102*, 132−145.

(7) Pinton, P.; Braicu, C.; Nougayrede, J. P.; Laffitte, J.; Taranu, I.; Oswald, I. P. Deoxynivalenol impairs porcine intestinal barrier function and decreases the protein expression of claudin-4 through a mitogen-activated protein kinase-dependent mechanism. *J. Nutr.* **2010**, *140*, 1956−1962.

(8) Ghareeb, K.; Awad, W. A.; Boehm, J.; Zebeli, Q. Impacts of the feed contaminant deoxynivalenol on the intestine of monogastric animals: poultry and swine. *J. Appl. Toxicol.* **2015**, *35*, 327−337.

(9) Paulick, M.; Rempe, I.; Kersten, S.; Schatzmayr, D.; Schwartz-Zimmermann, H. E.; Dänicke, S. Effects of increasing concentrations of sodium sulfite on deoxynivalenol and deoxynivalenol sulfonate concentrations of maize kernels and maize meal preserved at various moisture content. *Toxins* **2015**, *7*, 791−811.
(10) Yu, H.; Zhou, T.; Gong, J.; Young, C.; Su, X.; Li, X. Z.; Zhu, H.; Tsao, R.; Yang, R. Isolation of deoxynivalenol-transforming bacteria from the chicken intestines using the approach of PCR-DGGE guided microbial selection. *BMC Microbiol.* **2010**, *10*, No. 182.
(11) Li, P.; Su, R.; Yin, R.; Lai, D.; Wang, M.; Liu, Y.; Zhou, L. Detoxification of mycotoxins through biotransformation. *Toxins* **2020**, *12*, No. 121.
(12) Rempe, I.; Kersten, S.; Valenta, H.; Dänicke, S. Hydrothermal treatment of naturally contaminated maize in the presence of sodium metabisulfite, methylamine and calcium hydroxide; effects on the concentration of zearalenone and deoxynivalenol. *Mycotoxin Res.* **2013**, *29*, 169−175.
(13) Dänicke, S.; Hegewald, A. K.; Kahlert, S.; Kluess, J.; Rothkötter, H. J.; Breves, G.; Döll, S. Studies on the toxicity of deoxynivalenol (DON), sodium metabisulfite, DON-sulfonate (DONS) and de-epoxy-DON for porcine peripheral blood mononuclear cells and the intestinal porcine epithelial cell lines IPEC-1 and IPEC-J2, and on effects of DON and DONS on piglets. *Food Chem. Toxicol.* **2010**, *48*, 2154−2162.
(14) Dänicke, S.; Pahlow, G.; Beyer, M.; Goyarts, T.; Breves, G.; Valenta, H.; Humpf, H. U. Investigations on the kinetics of the concentration of deoxynivalenol (DON) and on spoilage by moulds and yeasts of wheat grain preserved with sodium metabisulfite ($Na_2S_2O_5$, SBS) and propionic acid at various moisture contents. *Arch. Anim. Nutr.* **2010**, *64*, 190−203.
(15) Schwartz, H. E.; Hametner, C.; Slavik, V.; Greitbauer, O.; Bichl, G.; Kunz-Vekiru, E.; Schatzmayr, D.; Berthiller, F. Characterization of three deoxynivalenol sulfonates formed by reaction of deoxynivalenol with sulfur reagents. *J Agric. Food Chem.* **2013**, *61*, 8941−8948.
(16) Frobose, H. L.; Fruge, E. D.; Tokach, M. D.; Hansen, E. L.; DeRouchey, J. M.; Dritz, S. S.; Goodband, R. D.; Nelssen, J. L. The influence of pelleting and supplementing sodium metabisulfite ($Na_2S_2O_5$) on nursery pigs fed diets contaminated with deoxynivalenol. *Anim. Feed Sci. Technol.* **2015**, *210*, 152−164.
(17) Dänicke, S.; Kersten, S.; Valenta, H.; Breves, G. Inactivation of deoxynivalenol-contaminated cereal grains with sodium metabisulfite: a review of procedures and toxicological aspects. *Mycotoxin Res.* **2012**, *28*, 199−218.
(18) Lasic, D. D. Novel applications of liposomes. *Trends Biotechnol.* **1988**, *16*, 307−321.
(19) Yang, X.; Liu, Y.; Yan, F.; Yang, C.; Yang, X. Effects of encapsulated organic acids and essential oils on intestinal barrier, microbial count, and bacterial metabolites in broiler chickens. *Poult. Sci.* **2019**, *98*, 2858−2865.
(20) Choi, J.; Wang, L.; Ammeter, E.; Lahaye, L.; Liu, S.; Nyachoti, M.; Yang, C. Evaluation of lipid matrix microencapsulation for intestinal delivery of thymol in weaned pigs. *Transl. Anim. Sci.* **2020**, *4*, 411−422.
(21) Tirosh, B.; Khatib, N.; Barenholz, Y.; Nissan, A.; Rubinstein, A. Transferrin as a luminal target for negatively charged liposomes in the inflamed colonic mucosa. *Mol. Pharm.* **2009**, *6*, 1083−1091.
(22) Barea, M. J.; Jenkins, M. J.; Lee, Y. S.; Johnson, P.; Bridson, R. H. Encapsulation of liposomes within pH responsive microspheres for oral colonic drug delivery. *Int. J. Biomater.* **2012**, *2012*, No. 458712.
(23) Yang, J.; Qiu, C.; Li, G.; Lee, W. J.; Tan, C. P.; Lai, O. M.; Wang, Y. Effect of diacylglycerol interfacial crystallization on the physical stability of water-in-oil emulsions. *Food Chem.* **2020**, *327*, No. 127014.
(24) How, C. W.; Rasedee, A.; Abbasalipourkabir, R. Characterization and cytotoxicity of nanostructured lipid carriers formulated with olive oil, hydrogenated palm oil, and polysorbate 80. *IEEE Trans. Nanobiosci.* **2012**, *12*, 72−78.
(25) Chime, S. A.; Onyishi, I. V. Lipid-based drug delivery systems (LDDS): recent advances and applications of lipids in drug delivery. *Afr. J. Pharm. Pharmacol.* **2013**, *7*, 3034−3059.
(26) Kenechukwu, F. C.; Attama, A. A.; Ibezim, E. C.; Nnamani, P. O.; Umeyor, C. E.; Uronnachi, E. M.; Momoh, M. A.; Akpa, P. A.; Ozioko, A. C. Novel intravaginal drug delivery system based on molecularly PEGylated lipid matrices for improved antifungal activity of miconazole nitrate. *BioMed Res. Int.* **2018**, *2018*, 1−18.
(27) Zhang, Y.; Wang, Q. C.; Yu, H.; Zhu, J.; De Lange, K.; Yin, Y.; Wang, Q.; Gong, J. Evaluation of alginate-whey protein microcapsules for intestinal delivery of lipophilic compounds in pigs. *J. Sci. Food Agric.* **2016**, *96*, 2674−2681.
(28) Wen, Z.; Xu, Z.; Zhou, Q.; Li, W.; Wu, Y.; Du, Y.; Chen, L.; Zhang, Y.; Xue, C.; Cao, Y. Oral administration of coated PEDV-loaded microspheres elicited PEDV-specific immunity in weaned piglets. *Vaccine* **2018**, *36*, 6803−6809.
(29) Young, J. C.; Trenholm, H. L.; Friend, D. W.; Prelusky, D. B. Detoxification of deoxynivalenol with sodium bisulfite and evaluation of the effects when pure mycotoxin or contaminated corn was treated and given to pigs. *J. Agric. Food Chem.* **1987**, *35*, 259−261.
(30) Mehnert, W.; Mäder, K. Solid lipid nanoparticles: production, characterization and applications. *Adv. Drug Delivery Rev.* **2012**, *64*, 83−101.
(31) Souto, E. B.; Müller, R. H. Lipid nanoparticles: effect on bioavailability and pharmacokinetic changes. *Drug Delivery* **2010**, 115−141.
(32) Hussain, A.; Samad, A.; Usman Mohd Siddique, M.; Beg, S. Lipid microparticles for oral bioavailability enhancement. *Recent Pat. Nanomed.* **2015**, *5*, 104−110.
(33) Bertoni, S.; Albertini, B.; Dolci, L. S.; Passerini, N. Spray congealed lipid microparticles for the local delivery of β-galactosidase to the small intestine. *Eur. J. Pharm. Biopharm.* **2018**, *132*, 1−10.
(34) Devreese, M.; Pasmans, F.; De Backer, P.; Croubels, S. An in vitro model using the IPEC-J2 cell line for efficacy and drug interaction testing of mycotoxin detoxifying agents. *Toxicol. In Vitro* **2013**, *27*, 157−163.
(35) Liao, P.; Liao, M.; Li, L.; Tan, B.; Yin, Y. Effect of deoxynivalenol on apoptosis, barrier function, and expression levels of genes involved in nutrient transport, mitochondrial biogenesis and function in IPEC-J2 cells. *Toxicol. Res.* **2017**, *6*, 866−877.
(36) Kamiloglu, S.; Sari, G.; Ozdal, T.; Capanoglu, E. Guidelines for cell viability assays. *Food Front.* **2020**, *1*, 332−349.
(37) Peskin, A. V.; Winterbourn, C. C. A microtiter plate assay for superoxide dismutase using a water-soluble tetrazolium salt (WST-1). *Clin. Chim. Acta* **2000**, *293*, 157−166.
(38) Lauren, D. R.; Smith, W. A. Stability of the Fusarium mycotoxins nivalenol, deoxynivalenol and zearalenone in ground maize under typical cooking environments. *Food Addit. Contam.* **2001**, *18*, 1011−1016.
(39) Wolf, C. E.; Bullerman, L. B. Heat and pH alter the concentration of deoxynivalenol in an aqueous enviroment. *J. Food Prot.* **1998**, *61*, 365−367.
(40) Mishra, S.; Dixit, S.; Dwivedi, P. D.; Pandey, H. P.; Das, M. Influence of temperature and pH on the degradation of deoxynivalenol (DON) in aqueous medium: comparative cytotoxicity of DON and degraded product. *Food Addit. Contam., Part A* **2014**, *31*, 121−131.
(41) Vandenbroucke, V.; Croubels, S.; Martel, A.; Verbrugghe, E.; Goossens, J.; Van Deun, K.; Boyen, F.; Thompson, A.; Shearer, N.; De Backer, P.; Haesebrouck, F. The mycotoxin deoxynivalenol potentiates intestinal inflammation by Salmonella typhimurium in porcine ileal loops. *PLoS One* **2011**, *6*, No. e23871.
(42) Wang, X.; Zhang, Y.; Zhao, J.; Cao, L.; Zhu, L.; Huang, Y.; Chen, X.; Rahman, S. U.; Feng, S.; Li, Y.; Wu, J. Deoxynivalenol induces inflammatory injury in IPEC-J2 cells via NF-κB signaling pathway. *Toxins* **2019**, *11*, No. 733.
(43) Zhang, H.; Deng, X.; Zhou, C.; Wu, W.; Zhang, H. Deoxynivalenol induces inflammation in IPEC-J2 cells by activating P38 MAPK and Erk1/2. *Toxins* **2020**, *12*, No. 180.

https://doi.org/10.1021/acsomega.1c00117
ACS Omega 2021, 6, 8382−8393

(44) Srinivasan, B.; Kolli, A. R.; Esch, M. B.; Abaci, H. E.; Shuler, M. L.; Hickman, J. J. TEER measurement techniques for in vitro barrier model systems. *J. Lab. Autom.* **2015**, *20*, 107−126.
(45) Peterson, L. W.; Artis, D. Intestinal epithelial cells: regulators of barrier function and immune homeostasis. *Nat. Rev. Immunol.* **2014**, *14*, 141−153.
(46) Beutel, O.; Maraspini, R.; Pombo-Garcia, K.; Martin-Lemaitre, C.; Honigmann, A. Phase separation of zonula occludens proteins drives formation of tight junctions. *Cell* **2019**, *179*, 923−936.
(47) Chen, Z.; Chen, H.; Li, X.; Yuan, Q.; Su, J.; Yang, L.; Ning, L.; Lei, H. Fumonisin B1 damages the barrier functions of porcine intestinal epithelial cells in vitro. *J. Biochem. Mol. Toxicol.* **2019**, *33*, No. e22397.
(48) Akbari, P.; Braber, S.; Gremmels, H.; Koelink, P. J.; Verheijden, K. A.; Garssen, J.; Fink-Gremmels, J. Deoxynivalenol: a trigger for intestinal integrity breakdown. *FASEB J.* **2014**, *28*, 2414−2429.
(49) Ma, T. Y.; Iwamoto, G. K.; Hoa, N. T.; Akotia, V.; Pedram, A.; Boivin, M. A.; Said, H. M. TNF-α-induced increase in intestinal epithelial tight junction permeability requires NF-κB activation. *Am. J. Physiol.: Gastrointest. Liver Physiol.* **2004**, *286*, G367−G376.
(50) Sadegh, C.; Schreck, R. P. The spectroscopic determination of aqueous sulfite using Ellman's reagent. *MURJ* **2003**, *8*, 39−43.
(51) Abràmoff, M. D.; Paulo, J. M.; Sunanda, J. R. Image processing with ImageJ. *Biophotonics Int.* **2004**, *11*, 36−42.
(52) Minekus, M.; Alminger, M.; Alvito, P.; Balance, S.; Bohn, T. O.; Bourlieu, C.; Carriere, F.; Boutrou, R.; Corredig, M.; Dupont, D.; Dufour, C. A standardised static in vitro digestion method suitable for food-an international consensus. *Food Funct.* **2014**, *5*, 1113−1124.
(53) Omonijo, F. A.; Kim, S.; Guo, T.; Wang, Q.; Gong, J.; Lahaye, L.; Bodin, J. C.; Nyachoti, M.; Liu, S.; Yang, C. Development of novel microparticles for effective delivery of thymol and lauric acid to pig intestinal tract. *J. Agric. Food Chem.* **2018**, *66*, 9608−9615.
(54) Livak, K. J.; Schmittgen, T. D. Analysis of relative gene expression data using real-time quantitative PCR and the 2-$\Delta\Delta$CT method. *Methods* **2001**, *25*, 402−408.
(55) Farkas, O.; Palócz, O.; Pászti-Gere, E.; Gálfi, P. Polymethoxyflavone apigenin-trimethylether suppresses LPS-induced inflammatory response in nontransformed porcine intestinal cell line IPEC-J2. *Oxid. Med. Cell. Longevity* **2015**, *2015*, No. 673847.
(56) Omonijo, F. A.; Liu, S.; Hui, Q.; Zhang, H.; Lahaye, L.; Bodin, J. C.; Gong, J.; Nyachoti, M.; Yang, C. Thymol improves barrier function and attenuates inflammatory responses in porcine intestinal epithelial cells during lipopolysaccharide (LPS)-induced inflammation. *J. Agric. Food Chem.* **2019**, *67*, 615−624.
(57) Yang, R.; Hui, Q.; Jiang, Q.; Liu, S.; Zhang, H.; Wu, J.; Lin, F.; Yang, C. Effect of Manitoba-grown red-osier dogwood extracts on recovering Caco-2 cells from H_2O_2-induced oxidative damage. *Antioxidants* **2019**, *8*, No. 250.
(58) Yu, C.; Li, Y.; Zhang, B.; Lin, M.; Li, J.; Zhang, L.; Wang, T.; Gao, F.; Zhou, G. Suppression of mTOR signaling pathways in skeletal muscle of finishing pigs by increasing the ratios of ether extract and neutral detergent fiber at the expense of starch in isoenergetic diets. *J. Agric. Food Chem.* **2016**, *64*, 1557−1564.

https://doi.org/10.1021/acsomega.1c00117
ACS Omega 2021, 6, 8382−8393